

An ENU-induced mutation in AP-2 α leads to middle ear and ocular defects in Doarad mice

Nadav Ahituv,^{1,*} Alexandra Erven,^{2,*} Helmut Fuchs,³ Keren Guy,¹ Ruth Ashery-Padan,¹ Trevor Williams,⁴ Martin Hrabe de Angelis,³ Karen B. Avraham,¹ Karen P. Steel^{2,†}

¹Department of Human Genetics and Molecular Medicine, Sackler School of Medicine, Tel Aviv University, Tel Aviv 69978, Israel

²MRC Institute of Hearing Research, University Park, Nottingham, UK

³GSF Research Center for Environment and Health, Institute of Experimental Genetics, Neuherberg, Germany

⁴Departments of Craniofacial Biology and of Cell and Structural Biology, University of Colorado Health Sciences Center, Denver, Colorado, 80262, USA

Received: 9 October 2003 / Accepted: 10 February 2004

Abstract

One of the advantages of *N*-ethyl- *N*-nitrosourea (ENU)-induced mutagenesis is that, after randomly causing point mutations, a variety of alleles can be generated in genes leading to diverse phenotypes. For example, transcription factor AP-2 α (*Tcfap2a*) null homozygote mice show a large spectrum of developmental defects, among them missing middle ear bones and tympanic ring. This is the usual occurrence, where mutations causing middle ear anomalies usually coincide with other abnormalities. Using ENU-induced mutagenesis, we discovered a new dominant *Tcfap2a* mutant named Doarad (*Dor*) that has a missense mutation in the PY motif of its transactivation domain, leading to a misshapen malleus, incus, and stapes without any other observable phenotype. *Dor* homozygous mice die perinatally, showing prominent abnormal facial structures and ocular defects. In vitro assays suggest that this mutation causes a "gain of function" in the transcriptional activation of AP-2 α . These mice enable us to address more specifically the developmental role of *Tcfap2a* in the eye and middle ear and are the first report of a mutation in a gene specifically causing middle ear abnormalities, leading to conductive hearing loss.

The embryological origin of the middle ear is diverse, since the middle ear and tympanic membrane arise from different developmental origins. The middle ear ossicles are formed from the first two branchial arches that originate from neural crest cells (NCC) that migrate from the developing mid-brain and hindbrain. The differentiation and survival of these cells in the branchial arches is thought to be mediated by the transcription factor AP-2 α (locus *Tcfap2a*), among others (Mallo 1998).

AP-2 α is a member of a family of transcription factors that function in a wide range of biological roles, including developmental processes, apoptosis, and cell cycle control (Hilger-Eversheim et al. 2000). It has a helix-span-helix motif in its C-terminal region that allows homodimerization while the basic helical DNA-binding motif enables binding to various GC-rich DNA sequences. Its N-terminal region is proline and glutamine rich and functions as a transcriptional activation region, and hence is named the transactivation domain.

Gene-targeted mutagenesis of the *Tcfap2a* gene leads to phenotypically normal heterozygous mice, except for 4% that show dental malocclusions (Zhang et al. 1996), while homozygous mice die perinatally, showing a wide range of severe developmental defects (Schorle et al. 1996; Zhang et al. 1996). The phenotype is first observed at embryonic day 9.5, with a failure in closure of the cranial neural folds that leads to anencephaly and missing ventral craniofacial structures such as a mouth, snout, or ears. *Tcfap2a* knockouts (*Tcfap2a*^{KO}) also have achordal skeleton defects with missing maxilla, cranial vault, middle ear bones, and tympanic ring. They also display other skeletal defects such as

*These authors contributed equally to this study.

†Present address: The Wellcome Trust Sanger Institute, Wellcome Trust Genome Campus, Hinxton, Cambridge, UK.

Correspondence to: Karen B. Avraham, E-mail: karena@post.tau.ac.il

scoliosis, a rib cage that fails to develop a medial sternum, missing clavicle, ocular defects, and limb defects with variable penetrance.

Since the knockouts showed severe and pleiotropic abnormalities, there was a need to study the individual defects caused by *Tcfap2a* in depth. Chimeric mice were generated that were composed of both wild-type and *Tcfap2a*-null cells (Nottoli et al. 1998). One of the phenotypes addressed using this technique was the ocular phenotype. In the eye, *Tcfap2a* is expressed early in ocular embryogenesis at embryonic day 9.5 in the developing lens (West-Mays et al. 1999). At embryonic day 15, AP-2 proteins are expressed in the developing lens, cornea, and retina, while AP-2 α is the only AP-2 protein expressed in the developing lens vesicle. Ocular phenotypes with variable defects in the developing eye were found in both *Tcfap2a* knockout and chimeric mice. The ocular phenotype ranged from complete lack of eyes (anophthalmia) to reduced size and shape of the lens, defects in the lens epithelium, failure of the lens to separate from the surface ectoderm, and development of neuroretina instead of anterior eye structures (West-Mays et al. 1999).

Here we report a new ENU-generated mouse mutant (Hrabe de Angelis et al. 2000) named Doard (*Dor*), exhibiting a "gain-of-function" missense mutation in the transactivation domain of AP-2 α . *Dor*+/ heterozygous mice have a misshapen malleus, incus, and stapes, leading to hearing impairment, without any other apparent phenotype. *Dor*/*Dor* homozygous mice die perinatally, exhibiting prominent facial defects and a severe ocular phenotype, with variable lens and retinal defects, coinciding with the *Tcfap2a* knockout and chimeric ocular phenotype.

Materials and methods

Mice and genotyping. The *Dor* mutation was generated in a large-scale ENU mutagenesis program in Neuherberg, Germany (Hrabe de Angelis et al. 2000). The colony was maintained at Tel Aviv University on a C3HeB/FeJ background. All experiments were carried out in full compliance with the Tel Aviv University Animal Care and Use Committee (M-00-65) and UK Home Office regulations. Genotyping was done using PCR primers 5'-CGATGGCGTGAGGTAAGGAGTG-3' and 5'-CCGACTTCCAGCC TCCACACTTC-3' that introduce a *Bsa*XI site only in PCR products encompassing the *Dor* mutation. *Tcfap2a*^{KO} mice were maintained on a Black Swiss background (Taconic) and were genotyped using PCR (Zhang et al. 1996). Embryos were taken from timed matings.

Auditory structure and function. Inner ears were cleared in methyl salicylate ($n = 6$ *Dor*+/+, 5 +/+), ossicles were dissected from the middle ear ($n = 26$ *Dor*+/+, 21 +/+), the organ of Corti was examined by scanning electron microscopy ($n = 10$ *Dor*+/+, 4 +/+), CAP thresholds and peak-to-peak amplitudes were measured from the round window using 2-dB steps ($n = 7$ *Dor*+/+ at 5–6 weeks, 5 at 4–5 months; +/+ 4 at 5–6 weeks, 5 at 4–5 months) and endocochlear potentials were measured using a micropipette electrode ($n = 12$ *Dor*+/+, 9 +/+), all as described previously (Steel and Smith 1992; Kiernan et al. 1999, 2002).

Mapping and sequence analysis. Mice were classified as +/+ or *Dor*+/+ by the presence or absence of an ear flick response (Preyer reflex). A custom-built click-box (MRC Institute of Hearing Research) was held 30 cm above the mouse and a calibrated 20-kHz toneburst at an intensity of 90 dB SPL was delivered. *Dor*+/+ mice on a C3HeB/FeJ genetic background were outcrossed to C57BL/6J mice and their mutant progeny were backcrossed to C3HeB/FeJ; backcrossing to C57BL/6J led to a reduction in the penetrance of the phenotype, making classification difficult. Only 55 mutants that could unequivocally be phenotyped as *Dor*+/+ by their phenotype were used for mapping. The entire genome was scanned as described previously (Kiernan et al. 1999) and additional chromosome 13 markers were used to narrow the region. cDNA generated from *Dor*+/+ brain RNA was used to sequence coding regions of candidate genes.

Histology and immunofluorescence analysis. Embryos were fixed in 1% paraformaldehyde (PFA) in PBS, embedded in paraffin, and sections stained using hematoxylin and eosin. For immunofluorescence, embryos were fixed in 4% PFA in PBS, embedded in paraffin, and performed on dewaxed paraffin sections after unmasking using the Antigen Unmasking Solution (Vector Lab, Burlingame, CA), blocking and washing as described (Ashery-Padan et al. 2000). The mouse anti-beta-III-tubulin (TUJ1) antibodies (Babco Covance, Princeton, NJ) were used at a dilution of 1:200, polyclonal AP-2 α antibodies (Santa Cruz Biotechnology Inc., Santa Cruz, CA) were used at a dilution of 1:100, and secondary antibodies were goat anti-mouse IgG rhodamine red-X conjugated (Jackson Immuno-Research Laboratories, West Grove, PA), at a dilution of 1:150. Nuclei were stained with 0.1 μ g/ml 4,6-diamidino-2-phenylindole (DAPI) (Sigma, St. Louis MO).

Cotransfection assays. Site-directed mutagenesis was performed based on the overlap extension PCR method (Pogulis et al. 1996) using the human

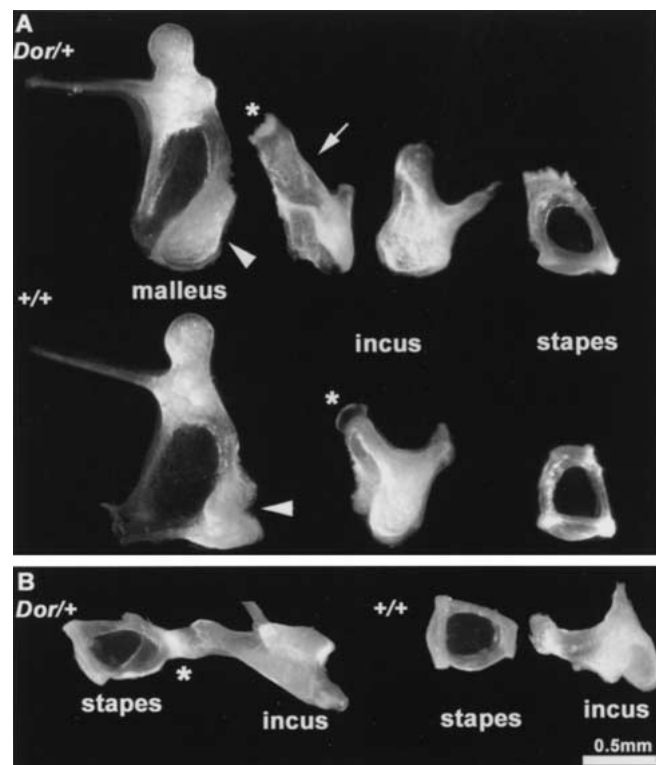


Fig. 1. Typical malformations in *Dor*/*+* ossicles. **(A)** Top row, *Dor*/*+*, bottom row, *+/+*. **(B)** Left, *Dor*/*+*, right, *+/+*. The *Dor*/*+* malleus has a flatter incudo-malleal joint (arrowhead) compared with the *+/+* malleus. Two examples of the *Dor*/*+* incus are shown in A: the shape is abnormal with a longer process in some (arrow) and a flatter joint. The *Dor*/*+* stapes is skewed in shape. The lenticular process is disc shaped in *+/+* mice (asterisk) but tendon-like in *Dor*/*+* mutants (asterisks in A and B).

TFAP2A expression construct SPRSV-AP2 (Williams and Tjian 1991) as template to generate the SPRSV-AP2 α P59L clone encompassing the *Dor* mutation. Transfections were performed in triplicate using Fugene 6 (Roche Applied Science, Indianapolis, IN) in HepG2 cells and LipofectamineTM (Invitrogen, Carlsbad, CA, MI) in NIH 3T3 cells. One microgram of each clone was transfected (mutant/wild-type 500 ng of each) along with 1 μ g of AP-2 α reporter construct p3 \times AP2-Bluc [a gift from Helen Hurst (Bamforth et al. 2001)] and 500 ng of pHM6-lacZ (Roche Applied Science), to correct for transfection efficiency. Activity of luciferase was measured using the Luciferase Assay System (Promega, Madison, WI) in the LUMAT LB9507 luminometer (EG&G Bertold, Australia).

Results

Middle ear defects in *Dor* heterozygous mutants. *Dor* heterozygotes show a weak or absent Preyer reflex, an ear flick response to a sudden sound,

Table 1. Ossicle defects in *Dor*/*+* mice^a

Ossicle	X ^b	X	\sqrt ^b	\sqrt
Malleus	X ^b	X	\sqrt ^b	\sqrt
Incus	X	X	X	\sqrt
Stapes	X	\sqrt	\sqrt	\sqrt
No. ears	30	3	1	11

^a 45 ears from 26 *Dor*/*+* mutants aged 20 days to 5 months, all genotyped by PCR. 27 ears from 21 *+/+* littermates showed minor anomalies only, as previously noted in C3H mice (Kiernan et al. 2002).

^b X = malformed, \sqrt = normal.

throughout life, with some variability between individuals. Examination of the gross structure of the inner ear was normal and there was no significant hair cell degeneration in adults, demonstrated by scanning electron microscopy (data not shown). Assessment of the middle ear ossicles (malleus, incus, stapes) of these mice revealed malformations. The malleus was narrower and the articulation with the incus was flatter than normal (Fig. 1A). The incus was distorted in shape, often appearing longer than normal and with a flattened incudo-malleal articulation. The incus was connected to the stapes through a broad tendonlike connection rather than the normal ossified lenticular process with a disc-shaped joint that characterizes the connection in normal mice (Fig. 1B). This tendonlike connection was soft and flexible when touched, suggesting that it would not act efficiently in transmitting vibration to the stapes. The stapes showed a slightly skewed shape in addition to its abnormal junction with the incus. Ossicle defects showed reduced penetrance and occasional asymmetry (Table 1).

Cochlear function was measured by recording compound action potentials (CAP) from the round window. Thresholds were raised by around 30 dB in *Dor*/*+* mutants aged 5–6 weeks and by 50 dB at 4–5 months compared with littermate controls (Fig. 2A). These elevations in threshold are within the range that might be predicted for a conductive hearing impairment (Browning and Gatehouse 1989), although there was no apparent reason for the deterioration in hearing with age. There was no unusual growth in the middle ears that was suggestive of otosclerosis, nor were there signs of inflammation to suggest otitis media. Waveforms of mutants were similar in shape to those of controls, with no sign of cochlear dysfunction (Fig. 2B). Endocochlear potentials of mutants were within the normal range, with a mean of 96.3 mV (range-88–106 mV) compared with 100.1 mV (range-92–104 mV) in controls, suggesting normal cochlear function. However, when CAP amplitudes were plotted with respect to stimulus intensity, the input/output functions normalized for differing thresholds would be expected to be similar in the two groups if there was a pure conductive component. There is broad overlap in these

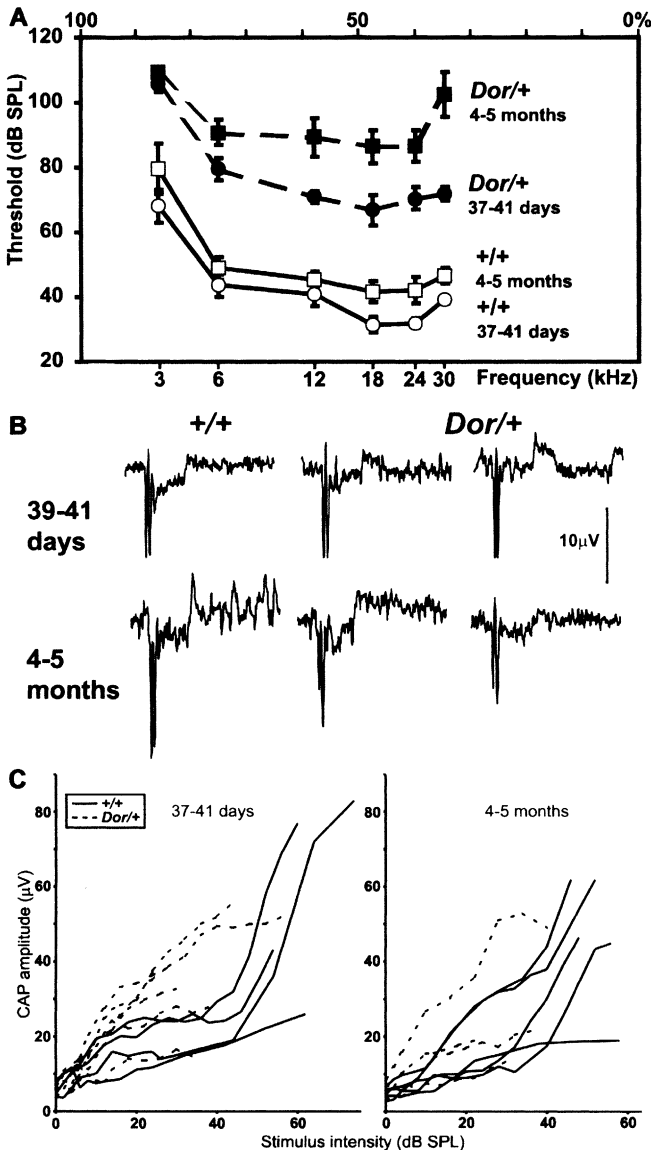


Fig. 2. (A) Mean (CAP) thresholds (with standard error bars) in *Dor*/*+* (filled symbols) and *+/+* (open symbols) mice. Scale at top indicates position along cochlear duct of best response to each frequency, where 0% is the base and 100% is the apex. (B) Some examples of CAP waveforms to illustrate their similar shape in *Dor* mutants and controls. Each waveform is the average of responses to 200 tonebursts at 18 kHz. Trace represents 50 ms, including 5 ms before tone onset, 15-ms tone duration, and the remainder shows the return to baseline noise levels. The CAP includes two sharp negative (downward) deflections, and some waveforms also show a sustained deflection (a summing potential) for the 15-ms toneburst duration. Amplitude scale bar is shown on the right. (C) CAP amplitudes in response to 18-kHz tonebursts at increasing stimulus intensity, normalized to the threshold of each mouse. Dashed lines represent individual *Dor*/*+* mice and solid lines *+/+* mice.

input/output functions in the 4–5-month old groups, but in the young group the mutant functions tend to

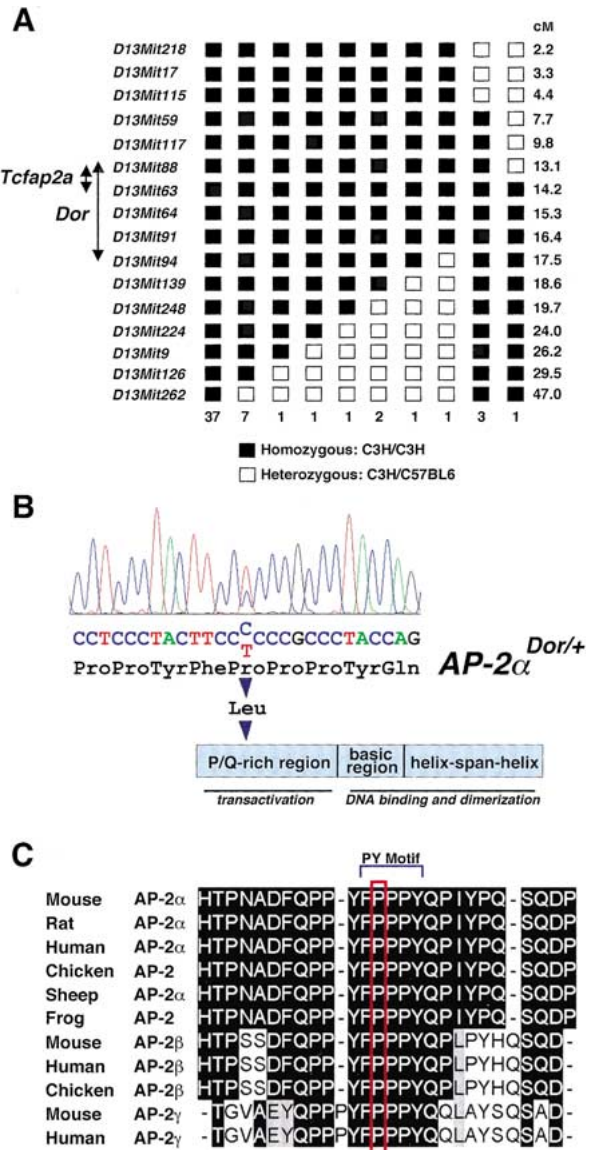


Fig. 3. *Dor* mapping and mutation analysis. (A) Allele distribution patterns of 55 backcross offspring. (B) Sequence of the *Tcfap2a* gene in a *Dor*/*+* mouse showing the C \rightarrow T mutation, the predicted protein sequence change, and its location in the schematic protein structure. (C) Amino acid sequence alignment of AP-2 molecules from various species, showing the conservation of this proline residue in vertebrates (red box).

rise more steeply, rather than showing the typical two-stage growth [slow growth followed by a steeper slope as intensity rises (Evans 1975)] (Fig. 2C). This indicates there may be a sensorineural component in addition to the conductive component of the hearing impairment.

Mapping and sequence analysis. *Dor* was mapped to a 4.4-cM region on mouse Chromosome 13 between markers *D13Mit88* and *D13Mit94*, located 13.1 and 17.5 cM, respectively, from the centromere

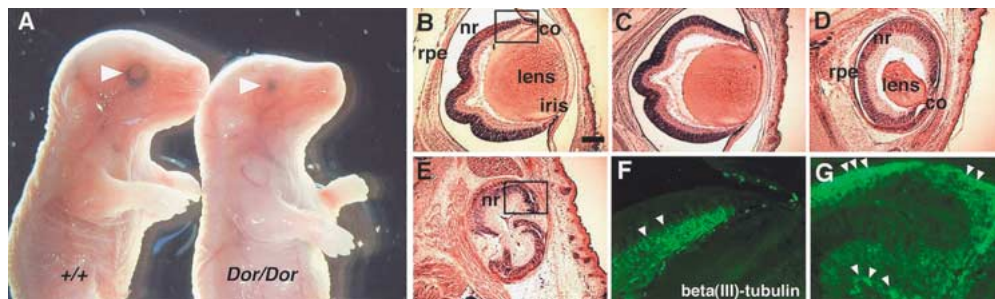


Fig. 4. *Dor/Dor* ocular phenotype. (A) Wild-type and *Dor/Dor* embryos at E18.5. The *Dor/Dor* embryos have smaller eyes (arrow) and abnormal facial structure in the form of a shorter and/or narrower snout. (B–E) H&E staining of sections of E18.5 eyes from wild-type (B), *Dor/+* (C), and *Dor/Dor* (D, E) embryos. (D, E) *Dor/Dor* mice show variability in ocular phenotype with adhesion of a smaller lens to the cornea (co) (D) or absence of lens (E). The neuroretina (nr) is folded in some embryos (E) and occasionally anterior eye structures, such as the iris, and ciliary body, fail to form and instead develop into a neuroretina (nr, E). (F, G) The tubulin isoform beta (III)-tubulin, a marker for postmitotic neurons, is detected (arrowheads) by immunostaining in the wild-type eye (F) in the differentiating neurons located in the inner layer of the optic cup. In the *Dor/Dor* mice (G), beta (III)-tubulin expression is evident in both inner and outer layers of the optic cup (arrowheads) in regions that normally develop into the ciliary body, iris, and pigmented epithelium. The section in F and G is adjacent to section B and E, respectively, and corresponds to boxed region in B and E. rpe, retinal pigmented epithelium. Scale bar: 200 μ m (B–E), 40 μ m (F, G).

(Fig. 3A). The following candidate genes in the region were selected for mutation screening based on their possible involvement in bone development: *msh-like 2* (*Msx2*), bone morphogenetic protein 6 (*Bmp6*), forkhead box C1 (*Foxc1*), barH-like homeobox 1 (*BarX1*), endothelin1 (*Edn1*), faciogenital dysplasia 3 (*Fgd3*), forkhead 10 (*Foxi1*), and AP-2 α (*Tcfap2a*).

Sequence analysis of the coding regions of the genes above, except for *Tcfap2a*, revealed no apparent nucleotide changes in *Dor* mice. In *Tcfap2a*, we discovered a C \rightarrow T missense mutation at position 246 (GenBank NM_011547), resulting in a nonconservative substitution of amino acid residue 59 (Swiss-Prot P34056), changing a proline to a leucine (P59L) (Fig. 3B). A comparison of AP-2 α with other transcription factors from the AP-2 family indicates that P59 is highly conserved, as it is part of the PY motif (Fig. 3C).

Ossicles in *Tafap2a*^{KO/+} mice. To ascertain whether the middle ear phenotype is distinctive to the *Dor* mice, we examined mice carrying one copy of a *Tcfap2a* knockout allele (Schorle et al. 1996; Zhang et al. 1996) and found that they had a normal Preyer reflex. The ossicles were mostly normal. Of 16 ears from 8 heterozygous mutants, one ear showed a slightly malformed incudo-malleal joint plus a lenticular process that was separated from the rest of the incus, and one stapes was solid with no hole between the two crura; all other ossicles were normal.

Homozygote phenotype of *Dor* mutants. Homozygous *Tcfap2a* knockout mice die perinatally, showing a wide range of severe developmental defects, such as neural tube, skeletal, body wall, sensory

organs, and limb defects, with variable penetrance (Schorle et al. 1996; Zhang et al. 1996). We were therefore interested in determining the phenotype of *Dor* homozygous mice. No live *Dor/Dor* mice were found in 7 litters examined ($n = 42$). We thus examined embryos at several developmental stages (E13.5–E18.5) and found a clear phenotype which differed from the homozygous knockout phenotype. *Dor* homozygous mice have very prominent abnormal facial structures, e.g., a shorter and/or narrower snout, compared with the wild-type mice and die perinatally (Fig. 4A). *Dor* homozygotes also show an abnormal developmental ocular phenotype, similar to the one described in *Tcfap2a*^{KO} and *Tcfap2a*^{KO} chimeric mice (West-Mays et al. 1999). Extreme variability in the ocular phenotype is observed with *Dor/Dor* mice (Table 2). The lens defects included reduced size, abnormal lens structure, and adhesions of the lens with the overlying surface ectoderm (Table 2, Fig. 4B–E). The retinal defects included folding of the retina (Fig. 4E), and, interestingly, in most mutants (66%) anterior eye structures derived from distal optic cup (ciliary-body, iris, pigmented epithelium) fail to form, but instead developed into neuroretina as indicated by the detection of the neuronal marker beta (III)-tubulin (Fig. 4F, G) in these cells. The similarity to the AP-2 α null phenotype supports the notion that *Dor* is a *Tcfap2a* allele.

Effect of *Dor* mutation on transcriptional activation. In order to assess the effects of the P59L mutation on the transcription activation properties of AP-2 α , we performed site-directed mutagenesis on the human AP-2 α expression construct, SPRSV-AP2 (Williams and Tjian 1991) to recreate the *Dor*

Table 2. *Dor* ocular phenotype

<i>Dor/Dor</i> age	<i>N</i> (eyes)	Normal lens	Abnormal lens	Absence of lens	Retinal abnormalities
E13.5	6	4	2	-	-
E16.5	6	-	6	-	1
E18.5	6	-	4	2	4

mutation. Since human and mouse AP-2 α have 98.85% protein identity, we reasoned that using a human AP-2 α expression construct would be adequate to simulate the *Dor* mutation. We conducted Western immunoblotting experiments using an AP-2 α -specific antibody 3B5 (Zhang et al. 1996) and confirmed protein overexpression of the mutant construct SPRSV-AP2 α P59L (data not shown). We then cotransfected cells with an AP-2 α reporter construct p3_XAP2-Bluc (including part of the c-erbB-2 promoter sequence, a known target for the AP-2 α transcription factor) (Bamforth et al. 2001; Bosher et al. 1996) and pHM6-lacZ (to correct for transfection efficiency) into HepG2 and NIH3T3 cells. HepG2 cells were chosen because of the absence of AP-2 α in this cell line (Williams and Tjian 1991). NIH 3T3 cells were chosen because of the previously described mutational and cotransfection studies carried out on this specific amino acid in these cells (Wankhade et al. 2000). In both cell lines, we observed an approximately twofold induction of luciferase activity in the mutant construct over and above that seen with the wild-type expression vector (Fig. 5). We also observed significantly higher induction levels in the mutant/wild-type cotransfec-

tions compared with the wild type. These results suggest that the *Dor* mutation causes a "gain-of-function" mutation in *Tcfap2a*, leading to increased transcriptional activation levels.

AP2 α expression in *Dor* mutants. AP-2 α expression was evaluated in order to determine levels of the protein in both *Dor* heterozygote and homozygote mice. In eyes of wild-type mice at age E13.5, AP2 α was found in the lens epithelium and in the cornea epithelium, as was also found previously (West-Mays et al. 1999). The expression pattern was similar in intensity and localization in *Dor*/+ mice and was detectable in *Dor/Dor* mice (Fig. 6). The similarity in expression levels further supports our hypothesis that the *Dor* mutation is a gain-of-function mutation.

Discussion

The middle ear transmits vibrations produced by the tympanic membrane in response to sound into the inner ear. In humans, disruption of this process as a result of bone dysplasia of the endochondral bone layer of the otic capsule (otosclerosis) or chronic otitis media often leads to hearing impairment in the form of conductive hearing loss (Declau and Van de Heyning 1996; Browning and Gatehouse 1989). The hearing impairment in *Dor* heterozygotes can be attributed largely to middle ear defects. The lack of a firm, ossified connection between the incus and stapes would severely impair the ability of the ossicular chain to transmit vibration to the inner ear, and the abnormal articulation between the malleus and incus may also impair conduction. We found no clear evidence of a cochlear defect, as endocochlear potentials were normal and there was little sign of hair cell degeneration, but we cannot rule out a sensorineural component to the hearing impairment because of the apparently steeper growth rate of CAP amplitudes with increasing stimulus intensity.

We have determined that the presence of a mutation, P59L, located in the transcriptional activation domain of the transcription factor AP-2 α correlates with the middle ear phenotype described in the Doarad mouse. We have several lines of evidence suggesting that the P59L *Tcfap2a* is the causative mutation. First, this proline resides in

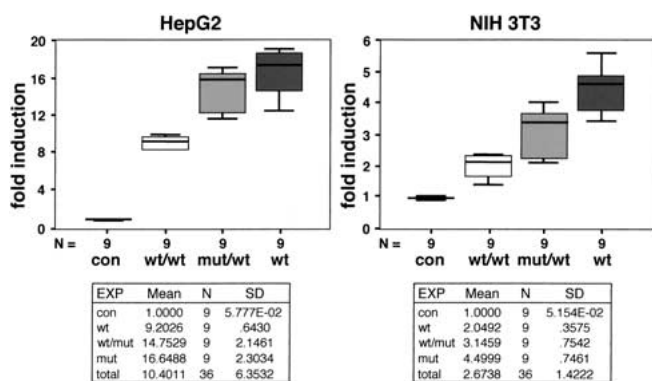


Fig. 5. Transcription activation of AP-2 α . Boxplots showing luciferase transcriptional activation levels, adjusted to the background levels of the transfected control construct SP(RSV)NN (black box). The boundaries of the boxes are the quartiles, the dark line inside them is the media, and extreme values are indicated by the vertical lines emerging from the boxes. Wild-type SPRSV-AP2, *Dor* mutant SPRSV-AP2 α P59L, and wild-type/mutant are shown. Tables summarize the mean and standard deviation of each experiment.

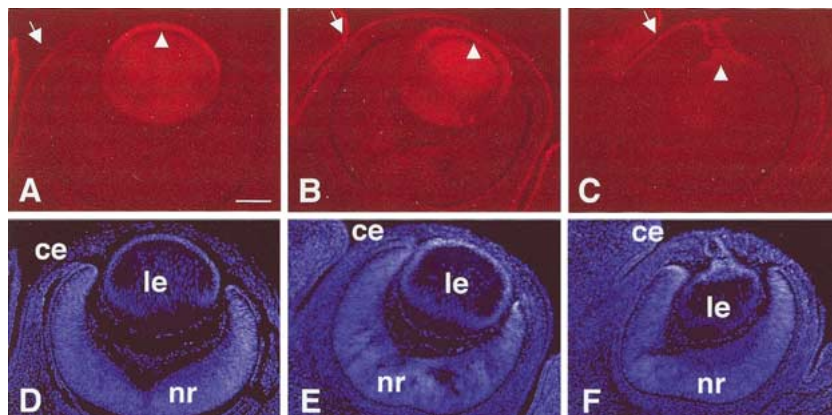


Fig. 6. AP2 α is detected in E13.5 *Dor* mutant mice. (A–C) AP2 α protein is detected in the lens epithelium (le; arrowhead) and in the cornea epithelium (ce; arrow) in E13.5 eyes of (A) wild-type, (B) *Dor*/+ and (C) *Dor*/*Dor* embryos. The *Dor*/*Dor* eyes are abnormal; the lens is smaller and attached to the cornea; nevertheless the AP2 α protein is detected in the remaining cells. (D–F) Counterstaining was done on the same sections with DAPI. nr, neuroretina. Scale bar: 100 μ m.

a highly conserved PY motif (Fig. 3D) found in all AP-2 homologs, except for the recently discovered AP-2 δ where the entire PY motif is absent (Zhao et al. 2001a). The PY motif is thought to be a binding site for transcriptional coactivators. This specific proline was changed to an alanine in an AP-2 α expression clone and cotransfected with an AP-2 reporter vector in NIH 3T3 cells, giving only 35% transcriptional activation when compared with wild-type clone, indicating that this amino acid is of importance to the PY motif (Wankhade et al. 2000). The *Dor* mutation was found to cause a two fold increase in expression activity in both NIH 3T3 and HepG2 cell assay, compared with wild type. These results suggest that alterations in this motif can subtly alter the properties of this transcriptional activation motif. Second, *Tcfap2a* homozygous knockouts showed missing middle ear bones and tympanic rings (Zhang et al. 1996) and a similar ocular phenotype as the *Dor* homozygous mice. Third, mutations in a member of the human AP-2 family, *TFAP2B*, were found to cause Char syndrome (MIM 169100), and one of these mutations is located in the third proline of the PY motif, leading to a mild form of Char syndrome (Zhao et al. 2001b). Fourth, expression studies correlate with the observed phenotype, finding *Tcfap2a* to be expressed starting at day 8–9 of mouse embryonic development in cranial neural crest cells (Mitchell et al. 1991), allowing the formation of the first two branchial arches which will later form the middle ear ossicles. The last additional line of evi-

dence comes from genetic studies in other vertebrate species. In humans, ear anomalies have been described in most of the distal 6p deletion syndromes identified and *TFAP2A* lies within the affected region (Law et al. 1998). More recently, studies in zebrafish have identified an AP-2 mutation that influences the development of the specific fish pharyngeal arches that in mammals give rise to the middle ear bones (Knight et al. 2003).

Dor homozygotes were found to have a milder phenotype than the *Tcfap2a*^{KO}/*Tcfap2a*^{KO}-mice. They die perinatally, showing prominent abnormal facial structure and variable ocular abnormalities. Variability in ocular phenotype also was observed in *Tcfap2a* knockout and chimeric mice (West–Mays et al. 1999), although *Dor*/*Dor* mice showed a milder phenotype (Table 3) (West–Mays et al. 1999). We did not observe any defects in cranial neural tube closure that led to anencephaly in the knockouts, nor did we see any failure in body wall closure.

The differences in phenotype between *Dor* mutants and the knockouts could be accredited to the effects of the specific ENU-generated missense mutation in *Dor* mice compared with the presumed absence of protein in the knockouts (Table 3). The milder homozygous *Dor* phenotype could be attributed to the location of the mutation in the transactivation domain, allowing homodimerization followed by DNA binding but leading to altered transcriptional activation. Our observations of enhanced transcriptional activation resulting from the

Table 3. Variability of phenotypes in relation to genotype

Genotype/phenotype	Middle ear abnormalities	Ocular phenotype	Failure cranial neural tube ^a	Lethality
<i>Dor</i> /+	X ^b	√ ^b	√	√
<i>Dor</i> / <i>Dor</i>	X	X	√	X
<i>Tcfap2a</i> ^{KO} /+	√	√	√	√
<i>Tcfap2a</i> ^{KO} / <i>Tcfap2a</i> ^{KO}	X	X	X	X

^a Includes body wall closure.

^b X = malformed, √ = normal.

Dor mutation support the suggestion of a different mode of action of the two types of mutations.

Because of the quantitative nature of transcription factor interactions, several gain-of-function mutations have been described in the literature as being associated with disease, skeletal malformation being no exception (reviewed in Hermanns and Lee 2001). One such example is *Msx2*, one of the candidates in the *Dor* mapped region. The loss or reduction in *Msx2* function leads to one class of defects in skull formation (parietal foramina) (Satokata et al. 2000), whereas a gain-of-function mutation or the overexpression of *Msx2* causes a second type, craniosynostosis (Liu et al. 1995). This gain-of-function mutation was shown to bind with higher affinity to several *Msx2* DNA target sequences, compared with the wild-type counterpart (Ma et al. 1996). These results indicate that a difference of phenotype can be associated with different mutations, one leading to gain of function while others may cause loss of function.

The PY motif is thought to bind to transcriptional coactivator proteins, most of which have not yet been characterized. The PY motif was originally identified by coprecipitation studies using the WW domain (Chen and Sudol 1995), a region of approximately 40 amino acids containing four highly conserved aromatic amino acids. It was found in a variety of proteins such as YAP, Nedd-4, Rsp5, Publ, dystrophin, FE65, and many more (Ilsley et al. 2002). Some of these proteins have been implicated in transcriptional regulation and YAP was shown to function as a transcriptional coactivator (Yagi et al. 1999). Cross-affinity experiments using peptides with different PY motifs, among them a peptide corresponding to transcription factor AP-2 α , showed differences in binding specificity to peptides corresponding to several WW domains, indicating a certain distinction of WW domains in terms of their binding partners (Pirozzi et al. 1997). It could very well be that the P59L mutation changes the specificity of this binding interaction, bringing about the *Dor* phenotype.

Several studies have identified a subset of transcriptional coactivators that can interact with transcription factor AP-2 α , although none of these interactions has as yet been mapped to the PY motif. The CBP/p300-interacting transactivator with ED-rich tails 2 and 4 (CITED2 and CITED4) were found to interact with transcription factor AP-2 α (Bamforth et al. 2001; Braganca et al. 2002). The CITED2 interaction domain maps to the C-terminal half of transcription factor AP-2 α while the CITED4 interaction domain is yet unknown (H.C. Hurst, personal communication). PC4, a transcriptional coactivator shown to stimulate transcriptional activation during TFIIA-TFIID-promoter complex for-

mation (Kaiser et al. 1995), is the only transcriptional coactivator found to interact with the N-terminal region/transactivation domain of transcription factor AP-2 α (Kannan and Tainsky 1999). Thus, it will be interesting to determine whether the *Dor* mutation affects the interaction between these transcription coactivators, particularly PC4.

A number of genes encoding transcription factors and signaling molecules have been shown to be involved in middle ear development, e.g., *Eyal*, *Prxl*, *Gsc*, *Dlx1-3*, *Hoxa1*, *Hoxa2*, *Fgf8* (reviewed in Mallo 1998), but *Dor* is the first mutant in which middle ear defects appear to be the only defect caused by the mutation in heterozygotes, showing the potential of ENU-induced mutants in discovering novel phenotypic alleles for different genes.

Acknowledgments

The authors thank Helen Hurst, Stephanie Donaldson, Hubert Schorle, Thomas Schilling, and Ori Brenner for reagents and advice. We would like to acknowledge Rudi Balling for his contribution to setting up the mutagenesis program. This work was supported by the Israel Ministry of Health (K.B.A.), the G.I.F., the German-Israeli Foundation for Scientific Research and Development (K.B.A. and M.H.d.A.), the European Economic Community (QLG2-CT-1999-00988 and BMH4-CT97-2715; K.B.A. and K.P.S.), the UK MRC and Defeating Deafness (K.P.S.), the Israel Science Foundation (401/02; R.A.-P.), and NIH grant DE12728 (T.W.).

References

1. Ashery-Padan R, Marquardt T, Zhou X, Gruss P (2000) Pax6 activity in the lens primordium is required for lens formation and for correct placement of a single retina in the eye. *Genes Dev* 14, 2701–2711
2. Bamforth SD, Braganca J, Eloranta JJ, Murdoch JN, Marques FI et al. (2001) Cardiac malformations, adrenal agenesis, neural crest defects and exencephaly in mice lacking *Cited2*, a new Tfp2 co-activator *Nat Genet* 29, 469–474
3. Boshier JM, Totty NF, Hsuan JJ, Williams T, Hurst HC (1996) A family of AP-2 proteins regulates c-erbB-2 expression in mammary carcinoma *Oncogene* 13, 1701–1707
4. Braganca J, Swingler T, Marques FI, Jones T, Eloranta JJ et al. (2002) Human CREB-binding protein/p300-interacting transactivator with ED-rich tail (CITED) 4, a new member of the CITED family, functions as a co-activator for transcription factor AP-2. *J Biol Chem* 277, 8559–8565
5. Browning GG, Gatehouse S (1989) Hearing in chronic suppurative otitis media. *Ann Oto Rhinol Laryngol* 98, 245–250

6. Chen HI, Sudol M (1995) The WW domain of Yes-associated protein binds a proline-rich ligand that differs from the consensus established for Src homology 3-binding modules *Proc Natl Acad Sci USA* 92, 7819–7823
7. Declau F, van de Heyning P (1996) Otosclerosis. In: Martini A, Read A, Stephens D (eds) *Genetics and Hearing Impairment*. London, UK, Whurr, pp 221–230
8. Evans EF (1975) The sharpening of cochlear frequency selectivity in the normal and abnormal cochlea *Audiology* 14, 419–442
9. Hermanns P, Lee B (2001) Transcriptional dysregulation in skeletal malformation syndromes. *Am J Med Genet* 106, 258–271
10. Hilger-Eversheim K, Moser M, Schorle H, Buettner R (2000) Regulatory roles of AP-2 transcription factors in vertebrate development, apoptosis and cell-cycle control. *Gene* 260, 1–12
11. de Hrabe Angelis MH, Flaswinkel H, Fuchs H, Rathkolb B, Soewarto D et al. (2000) Genome-wide, large-scale production of mutant mice by ENU mutagenesis. *Nat Genet* 25, 444–447
12. Ilsley JL, Sudol M, Winder SJ (2002) The WW domain: linking cell signalling to the membrane cytoskeleton. *Cell Signal* 14, 183–189
13. Kaiser K, Stelzer G, Meisterernst M (1995) The coactivator p15 (PC4) initiates transcriptional activation during TFIIA–TFIID-promoter complex formation. *EMBO J* 14, 3520–3527
14. Kannan P, Tainsky MA (1999) Coactivator PC4 mediates AP-2 transcriptional activity and suppresses ras-induced transformation dependent on AP-2 transcriptional interference. *Mol Cell Biol* 19, 899–908
15. Kiernan AE, Zalzman M, Fuchs H, Hrabe de Angelis MH, Balling R et al. (1999) Tailchaser (*Tlc*): a new mouse mutation affecting hair bundle differentiation and hair cell survival. *J Neurocytol* 28, 969–985
16. Kiernan AE, Erven A, Voegeling S, Peters J, Nolan P et al. (2002) ENU mutagenesis reveals a highly mutable locus on mouse Chromosome 4 that affects ear morphogenesis *Mamm Genome* 13, 142–148
17. Knight RD, Nair S, Nelson SS, Afshar A, Javidan Y et al. (2003) Lockjaw encodes a zebrafish *tfap2a* required for early neural crest development. *Development* 130, 5755–5768
18. Law CJ, Fisher AM, Temple IK (1998) Distal 6p deletion syndrome: a report of a case with anterior chamber eye anomaly and review of published reports. *J Med Genet* 35, 685–689
19. Liu YH, Kundu R, Wu L, Luo W, Ignelzi MA Jr, et al. (1995) Premature suture closure and ectopic cranial bone in mice expressing *Msx2* transgenes in the developing skull. *Proc Natl Acad Sci USA* 92, 6137–6141
20. Ma L, Golden S, Wu L, Maxson R (1996) The molecular basis of Boston-type craniosynostosis: the Pro148 → His mutation in the N-terminal arm of the *MSX2* homeodomain stabilizes DNA binding without altering nucleotide sequence preferences. *Hum Mol Genet* 5, 1915–1920
21. Mallo M (1998) Embryological and genetic aspects of middle ear development. *Int J Dev Biol* 42, 11–22
22. Mitchell PJ, Timmons PM, Hebert JM, Rigby PW, Tjian R (1991) Transcription factor AP-2 is expressed in neural crest cell lineages during mouse embryogenesis. *Genes Dev* 5, 105–119
23. Nottoli T, Hagopian-Donaldson S, Zhang J, Perkins A, Williams T (1998) AP-2-null cells disrupt morphogenesis of the eye, face, and limbs in chimeric mice. *Proc Natl Acad Sci USA* 95, 13714–13719
24. Pirozzi G, McConnell SJ, Uveges AJ, Carter JM, Sparks AB et al. (1997) Identification of novel human WW domain-containing proteins by cloning of ligand targets. *J Biol Chem* 272, 14611–14616
25. Pogulis RJ, Vallejo AN, Pease LR (1996) In vitro recombination and mutagenesis by overlap extension PCR. In: Trower MK (ed.) *In vitro mutagenesis protocols*. Totowa, NJ, Humana Press Inc, pp 167–176
26. Satokata I, Ma L, Ohshima H, Bei M, Woo I et al. (2000) *Msx2* deficiency in mice causes pleiotropic defects in bone growth and ectodermal organ formation. *Nat Genet* 24, 391–395
27. Schorle H, Meier P, Buchert M, Jaenisch R, Mitchell PJ (1996) Transcription factor AP-2 essential for cranial closure and craniofacial development. *Nature* 381, 235–238
28. Steel KP, Smith RJ (1992) Normal hearing in *Sp/+*, the mouse homologue of Waardenburg syndrome type 1. *Nat Genet* 2, 75–79
29. Wankhade S, Yu Y, Weinberg J, Tainsky MA, Kannan P (2000) Characterization of the activation domains of AP-2 family transcription factors. *J Biol Chem* 275, 29701–29708
30. West-Mays JA, Zhang J, Nottoli T, Hagopian-Donaldson S, Libby D et al. (1999) AP-2alpha transcription factor is required for early morphogenesis of the lens vesicle. *Dev Biol* 206, 46–62
31. Williams T, Tjian R (1991) Analysis of the DNA-binding and activation properties of the human transcription factor AP-2 *Genes Dev* 5, 670–682
32. Yagi R, Chen LF, Shigesada K, Murakami Y, Ito Y (1999) A WW domain-containing yes-associated protein (YAP) is a novel transcriptional co-activator. *EMBO J* 18, 2551–2562
33. Zhang J, Hagopian-Donaldson S, Serbedzija G, Elsemore J, Plehn-Dujowich D et al. (1996) Neural tube, skeletal and body wall defects in mice lacking transcription factor AP-2. *Nature* 381, 238–241
34. Zhao F, Satoda M, Licht JD, Hayashizaki Y, Gelb BD (2001a) Cloning and characterization of a novel mouse AP-2 transcription factor, AP-2delta, with unique DNA binding and transactivation properties. *J Biol Chem* 276, 40755–40760
35. Zhao F, Weismann CG, Satoda M, Pierpont ME, Sweeney E et al. (2001b) Novel TFAP2B mutations that cause Char syndrome provide a genotype-phenotype correlation. *Am J Hum Genet* 69, 695–703